Published in final edited form as:
Cytotherapy. 2013 February ; 15(2): 171–184.e1. doi:10.1016/j.jcyt.2012.11.006.

Analysis of chemotactic molecules in bone marrow-derived mesenchymal stem cells and the skin: Ccl27-Ccr10 axis as a basis for targeting to cutaneous tissues

Vitali Alexeev[1], **Adele Donahue**[1], **Jouni Uitto**[1], and **Olga Igoucheva**[1]
[1]Department of Dermatology and Cutaneous Biology, Jefferson Medical College, Thomas Jefferson University, 233 South 10th Street, Philadelphia, PA 19107

Abstract

Background aims—The adult stem cells produce a plethora of extracellular matrix (ECM) molecules and have a high potential as cell-based therapeutics for connective tissue disorders of the skin. However, the primary challenge of the stem cell-based approach is associated with the inefficient homing of systemically infused stem cells to the skin.

Methods—We examined chemotactic mechanisms that govern directional migration of the mesenchymal stem cells (MSCs) into the skin by conducting a comprehensive expression analysis of chemotactic molecules in MSCs and defined cutaneous tissues from normal and hereditary epidermolysis bullosa (EB)-affected skin.

Results—Analysis of chemokine receptors in short and long-term MSC cultures showed tissue culture-dependent expression of several receptors. Assessment of epidermis- and dermis-derived chemokines showed that majority of skin-originated chemotactic signals preferentially recruit different sets of leukocytes rather than MSCs. Analysis of the chemotactic molecules derived from EB-affected non-blistered skin showed only minor changes in expression of selected chemokines and receptors. Nevertheless, the data allowed us to define Ccl27-Ccr10 chemotactic axis as the most potent for the recruitment of MSCs to the skin. Our in vivo analysis demonstrated that uniform expression of Ccr10 on MSCs and alteration of Ccl27 level in the skin enhance extravasation of stem cells from circulation and facilitate their migration within cutaneous tissue.

Conclusions—Collectively, our study provides a comprehensive analysis of chemotactic signal in normal and EB-affected skin and proof-of-concept data demonstrating that alteration of the chemotactic pathways can enhance skin homing of the therapeutic stem cells.

Keywords

Adult stem cells; Mesenchymal stem cells; Migration; Gene expression analysis; Chemokines; Chemokine receptors; Blistering skin; Epidermolysis bullosa; Transplantation

Correspondence should be addressed: Olga Igoucheva, Ph.D., Department of Dermatology and Cutaneous Biology, Jefferson Medical College, Thomas Jefferson University, 233 South 10th Street, BLSB, Rm. 430, Philadelphia, PA 19107, (Tel) 215-503-5434, (Fax) 215-503-5788, Olga.Igoucheva@jefferson.edu.

Disclosure of interests
The authors indicate no potential conflicts of interest.

Introduction

Adult bone marrow-derived mesenchymal stem cells (MSCs) have shown great promise for their potential in developing cell-based therapies for the treatment of acquired and genetic disorders and as a tool for regenerative therapy (1). Nevertheless, effective engraftment of the transplanted MSCs into affected tissue after systemic introduction remains a major limitation. Homing of transplanted MSCs into injured tissue is regulated by multiple processes, including cell recruitment, migration and adhesion. Although the molecular mechanisms that govern directional migration of the MSCs are not fully understood, there is an accumulating body of evidence that chemotaxis plays a crucial role in homing of circulating MSCs to peripheral tissues. Chemotactic process depends on the signaling protein molecules, chemokines, which are secreted from the tissues and activate specific G-protein coupled chemokine receptors on the surface of rolling cells in circulation. Interaction between chemokines and their respective receptors leads to multiple intracellular events that allow extravasation of cells from circulation and directional migration towards the area with the highest chemotactic gradient. A complete understanding of the mechanisms that enhance MSCs migration in injured tissue, therefore, is critical for improving their repair capacity and therapeutic application.

Since MSCs are naturally involved in the regeneration/repair of multiple tissues, a number of studies examined expression of chemokine receptors in MSCs. It has been reported that human and mouse MSCs express low levels of selected chemokines and receptors (2–4); however, responsiveness of MSCs to only a few chemokines has been experimentally tested. For example, it has been shown that mouse MSCs respond by directional migration to CCL21 (5). When this recombinant chemokine was injected intradermally into wounded mouse skin, a slightly elevated number of transplanted MSCs migrated toward the injection site. Directional migration of the MSCs toward CCL25, the only known ligand for the CCR9, was also shown in an in *vitro* assay (6). As CCL25 is one of the major chemokines expressed in intestine and thymus, it is plausible that $CCR9^+$ MSCs are preferentially recruited to these organs. Yet, no direct *in vivo* conformation is available to prove this hypothesis. Another recent study showed that human MSCs can also respond *in vitro* to CXCL7, a known ligand for CXCR2 (7). Because MSCs express CXCR4, which provides retention of stem cells in CXCL12-expressing bone marrow, it was suggested that migration of $CXCR4^+$ MSCs could be directed to specific sites in the body by CXCL12. For example, engineered MSCs constitutively expressing CXCR4 were shown to home to the myocardium *in vivo* on experimental rat infarction model and protect myocardium from wall thinning (8). It was also shown that CXCR4 overexpressing MSCs readily engrafted into irradiated enteric mucosa due to the naturally high CXCL12 expression in irradiated intestine and ameliorated intestinal permeability and histopathological damage (9).

Further examination of molecular mechanisms that provide chemotactic attraction of MSCs showed that exposure of these cells to CCL25, CXCL7, CXCL12 leads to significant induction of genes involved in chemotaxis, homing, cytoskeletal and membrane reorganization, cell–matrix interaction, and cell motility (6, 7, 10). Significant up-regulation of interleukin 6 (IL6), interleukin 8 (IL8, CXCL8) and leukocyte inhibitory factor (LIF) was also observed. Another recent study showed that in MSCs exposed to chemokines CCL5 and CXCL12 differential activation of signal transducer and activator of transcription (STAT) proteins was observed (3).

Involvement of MSCs in skin wound repair has also been examined by injecting them into periphery of wounds or by applying them directly to the wound bed. These applications were shown to significantly accelerate re-epithelialization, angiogenesis and wound closure (11). It is conceivable that MSCs can facilitate these processes due to secretion of various

paracrine signaling molecules, such as VEGF, IGF-1, EGF, KGF, SDF-1, CCL3,3 angiopoietin-1 and erythropoietin (12, 13). However, it was also shown that directional migration and homing of endogenous MSCs to the skin is not particularly efficient in physiological and pathological conditions (13). Even intravenous injection of MSCs into mice with skin wounds showed only transient accumulation of infused MSC to the wounded skin during first 3 days but that was followed by rapid loss of stem cells from the lesion during subsequent 3–5 days (5).

Collectively, these studies indicated that recruitment of circulating MSCs to affected tissues is tightly controlled by chemokines and suggested that limited homing of MSCs to the homeostatic and wounded skin may result from the inefficacy of appropriate chemotactic signals that facilitate homing of adult progenitor cells to the skin. To experimentally test this hypothesis, we examined expression of chemokines in normal skin as well as in and diseased skin characterized by the disrupted dermal-epidermal junction and blistering. We also analyzed expression of chemokine receptors in minimal and prolonged MSCs cultures, and defined appropriate chemotactic axis that can be utilized for the efficient recruitment of therapeutic MSCs to the skin for the treatment of acquired and hereditary cutaneous disorders.

Materials and Methods

Mouse strains

Wild-type C57BL/6 mice were purchased from The Jackson Laboratory (Bar Harbor, ME). Transgenic type VII collagen-deficient (*Col7a1*$^{-/-}$) and laminin γ2-deficient (*Lamc2*$^{-/-}$) mice were generated in the Department of Dermatology and Cutaneous Biology, Thomas Jefferson University (14, 15). Transgenic laminin β3-deficient mice (*Lamb3*^{IAP66}) were obtained from Wadsworth Center State of New York Department of Health (16).

Preparation of primary cells and tissue culture conditions

Primary bone marrow-derived MSCs were isolated from newborn C57BL/6 wild-type mice as described previously (17). Immunodepletion was carried out using mouse lineage depletion kit (Miltenyi Biotec, Auburn, CA). MSCs were cultured in MesenCult Growth Media with supplements (StemCell Technologies, Vancouver, BC, Canada). For isolation of skin-derived layers as well as resident keratinocytes and fibroblasts, newborn mice were euthanized by CO_2 inhalation and disinfected by consecutively washing with Betadine Solution™ (Purdue Products L.P., Stamford, CT), 70% ethanol and Hanks' balanced salt solution (HBSS) supplemented with penicillin/streptomycin. After removal of limbs, tail and head, an incision was made on the ventral side of the body, through the skin but not the peritoneum, and the epidermal layer was carefully pulled off the torso with forceps. To separate the epidermis in wild-type skin, biopsy was subjected to the proteolytic digestion with mixture of collagenase I, Dispase II, and DNase I at 37°C for 1 hr with vigorous agitation to digest collagenous matrix. After separation, entire epidermis was placed into a 500 μl drop of TrypLE Select (Invitrogen, Carlsbad, CA) in a culture dish with the basal layer downward. After 30 min of incubation at room temperature, a drop of CnT-7 culture media (Zenbio, Inc., Research Triangle Park, NC) was added onto the epidermis and single cells were separated from the epidermal sheet by gentle rubbing. Single cell suspension then was filtered through a 70 μm mesh and collected by centrifugation in CnT-7 media. For culturing, epithelial keratinocytes were maintained in CnT-7 media on gelatinized tissue culture plates. For isolation of the dermal component, the remaining skin was cleaned of the muscle and fat tissues and dermal layer was cut into small pieces. For primary culture of fibroblasts, dermal pieces were kept in DMEM/F12 supplemented with 10% FBS (Invitrogen, Carlsbad, CA) for 5 days, after which point tissue pieces were removed and

fibroblasts were collected by trypsinization for further propagation. In all cases, cells on early passages (p2–4) were used in experimentation unless stated otherwise. All primary cells were cultured at 37°C in a humidified 5% CO_2-95% air atmosphere.

Microarray and RT-PCR analyses

Oligo GE Mouse Chemokines and Receptors Array (SABiosciences) consisting of 114 related genes was used. The total RNA was extracted using the Qiagen RNAeasy extraction kit (Valencia, CA). For cRNA probe synthesis, 2 μg of total RNA was amplified and labeled using TrueLabeling-AMP 2.0 kit (SABiosciences, Frederick, MD). All steps including amplification, labeling and hybridization were performed according to the manufacturer's protocol (SABiosciences). Exposure time of hybridized membranes was adjusted so that the extent of hybridization was in a linear range. Acquisition of hybridization signals was quantitatively determined using the GEArray Expression Analysis Suite 2.0 software (SABiosciences), which reads the hybridization images and matches them to the corresponding gene on the array. Net expression of each gene was calculated by the mean intensity of the gene hybridization intensity minus the mean of the control or background intensity. To provide normalization, the average ratio of expression levels of two principal genes (GAPDH and β-actin) was determined and introduced as a correction factor. A 2-fold difference in expression was considered as significant. Reverse-transcription coupled with a polymerase chain reaction (RT-PCR) was used to confirm microarray data. Reaction was carried out using one-step RT-PCR kit (ABgene Inc, Rockford, IL) according to the manufacturer's protocol. All primers were purchased from Eurofins MWG Operon (Huntsville, AL) and their sequences are presented in Supplementary Table S1. For densitometric analysis, the signal intensities of RT-PCR products were quantitated with Quantity One software (Bio-Rad, Hercules, CA).

Fluorescence-activated cell sorting analysis (FACS)

Receptor expression in primary MSC cultures was determined via FACS using fluorescent-labeled antibodies generated against Ccr3, Ccr4, Ccr5, Ccr6, Ccr7, Ccr9, Ccr10, Cxcr2, Cxcr3, Cxcr4, Cxcr7 (BioLegend, San Diego, CA) as described previously (17). Cells labeled with FITC-, PE-, PerCp/Cy5.5- or Alexa Fluor-647-conjugated antibodies were analyzed with BD FACSCalibur flow cytometer (BD Biosciences). All measurements were analyzed with FlowJo analytical software (Ashland, OR).

Generation and characterization of Ccr10-overexpressing MSCs

Full-length mouse Ccr10 receptor with 3′ UTR was amplified from total mouse RNA via RT reaction using Superscript II RT Kit (Invitrogen) followed by PCR using PFU II high fidelity polymerase (Stratagene). Resultant cDNA was inserted into pEF2-TOPO vector. Integrity of the promoter and cDNA was verified by direct DNA sequencing. Minimally cultured MSCs (passage 1–2) were nucleofected with resultant plasmid (pEF1-mCcr10) using Lonza nucleofection reaction (T-27 program, nucleofection kit V). Further, pool of Ccr10-expressing cells was selected with Blasticidin (0.5 mg/ml) for ten days. Expression of Ccr10 in selected cells was confirmed by RT-PCR, Western blot and indirect immunofluorescence analyses. For Western blot, nuclear proteins were isolated using NE-PER Nuclear and Cytoplasmic Extraction kit (Pierce, Rockford, IL). Proteins were separated by a 4–12% gradient SDS-PAGE and transferred to PVDF membrane followed by the blot using polyclonal anti-Ccr10 antibodies (ThemoScientific). Immunocomplexes were detected by using HRP labeled anti-rabbit secondary antibodies (Promega, Madison, WI) and visualized by using SuperSignal WestFemto substrates (Pierce, Rockford, IL). For indirect immunofluorescence, Ccr10-immunocomplexes were detected with Alexa-Fluor^{594}-conjugated secondary antibodies (Invitrogen). Nuclei were counterstained with 46-

diamidino-2-phenyl indol (DAPI; Sigma, St. Louis, MO). Immunofluorescent images were obtained on Nikon TS100F fluorescent microscope.

Labeling and transplantation of MSCs into mice

All animal procedures were performed in accordance with the *Guide for the Care and Use of Laboratory Animals* (National Institutes of Health [NIH] publication No. 86-23) and approved by the Institutional Animal Care and Use Committee of the Thomas Jefferson University. Prior to transplantation, MSC^{min} and MSC^{Ccr10} cells were labeled overnight with $DiOC_{18}$ (green) and FM-DiI (red) cell tracer dyes (Invitrogen), respectively, as described previously (17). For local transplantation, a mixture of MSC^{min} and MSC^{Ccr10} cells (0.5×10^6 cells in 50 μl PBS; 1:1 ratio) or MSC^{Ccr10} (0.5×10^6 cells in 50 μl PBS) cells alone were injected intradermally (ID) into the dorsal skin of syngenic C57BL6/J mice (n=5/time point) depilated prior to transplantation. For systemic transplantation, the wild-type mice (n=5/time point) received FM-DiI-MSC^{min} and FM-DiI-MSC^{Ccr10} cells (1×10^6 cells in 200–250 μl PBS per mouse) through the lateral tail vein, respectively. To provide constant chemotactic gradient, 0.5 μg of recombinant mouse Ccl27 (R&D Systems, Minneapolis, MN) was injected ID at a distal site from cell infusion site (~2 cm) every two days. For direct viewing, transplanted cells were detected using IVIS live-imaging system (IVIS Lumina XR, Caliper LifeSciences). To avoid detection of auto-fluorescence from hairs, all experimental mice were depilated prior to imaging and exposure time was minimized to a maximum of 1 sec. All collected skin biopsies were embedded into OCT compound (VWR, Pittsburgh, PA), frozen, and cryosectioned at a thickness of 7 μm. For histological analysis, sections were stained with DAPI (Sigma) using a standard protocol. For analysis of cell engraftment, the entire skin biopsy containing engrafted FM-DiI-labeled cells was subjected to the proteolytic digestion with mixture of collagenase I, Dispase II, and DNase I followed by fluorescence-activated sorting of FM-DiI-positive MSCs from single-cell suspension as described previously (17).

Results and Discussion

Gene expression profile of chemokines and chemokine receptors in mouse MSCs

Several studies have reported expression of various chemokine receptors by human and mouse MSCs (4, 5, 18). However, multiple inconsistencies observed in these studies have been attributed to variations in methods of MSCs isolation, culture conditions, and detection of chemokine receptor expression. Having established rapid and reproducible method of MSCs isolation with pre-defined phenotypes (17), we examined expression of chemokines and chemokine receptors in minimally cultured MSCs (MSC^{min}) and MSCs after prolonged (>10 passages) culturing (MSC^{cult}). Initial array-based assessment of receptor expression showed that MSC^{min} and MSC^{cult} share similar expression pattern, however, several receptors, such as Ccr1, Ccr2, and Cxcr4, were expressed at higher level in MSC^{min} than in MSC^{cult} (Table 1). Analysis of chemokine expression showed that both cultures also express high level of several ligands, including Ccl1, Ccl2, Ccl5 Cxcl4 Cxcl14, and Cxc3cl1 (Table 1). Interestingly, Ccl19 and Ccl24 were expressed exclusively in MSC^{min}, whereas a very lower level of Ccl20 expression was detected only in MSC^{cult}.

The expression profile of selected chemokines and receptors in MSC^{min} was further verified by semi-quantitative RT-PCR using gene-specific primers and compared with that of the MSC^{cult}. Based on this analysis, MSC^{min} express high levels of Ccr1, Ccr2, Ccr7, Ccr10, Ccrl1, and Cscr4, consistent with gene array data. However, extended culturing led to a significant down-modulation of Ccr1, Ccr2, Ccr7 and Cxcr4 expression (Fig. 1A). In addition, expression of Ccr10 was slightly up-regulated in MSC^{cult}, whereas Ccrl1 remained unchanged. Prolong culturing also resulted in reduced expression of Ccl19, Ccl24 and

Cxcl4. Surprisingly, Ccl20, Ccl27, Cxcl12, Cx3cl1 and Il-18 were up-regulated in MSC^{cult}, whereas expression of Ccl2 and Ccl5 remained unchanged upon culturing.

Considering prior observations that chemokine receptors are not expressed uniformly in MSCs and that only limited yet uncharacterized subsets of MSCs express specific receptors, we further examined MSC^{min} and MSC^{cult} populations for the expression of selected receptors at protein level via FACS analysis. Although this analysis was limited by the availability of receptor-specific antibodies, it was observed that more than 60% on MSC^{min} expressed low level of Ccr6, whereas 16% of cells were highly positive for Cxcr4 and 14% for Ccr10. Fifteen to 20 % of ^{min} population was also positive for Ccr4 and Cxcr3 (Fig. 1C). For the majority of chemokine receptors, our data are in good correlation with prior findings (4, 18). However, relatively high level of Ccr9 protein reported previously (19) was not observed in our analyses. After prolonged culturing, MSCs continue to express majority of identified chemokine receptors, however, several differences were observed (Fig. 1C, Table 1). Thus, after extended culturing higher percentage of MSCs expressed Ccr4, Ccr7, Ccr9, Cxcr2, and Cxcr7, whereas Ccr6, Cxcr4 and Cxcr3 were expressed in lesser number of cells. Although level of Ccr10 expression in cultured MSCs increased with passages, as determined by semi-quantitative RT-PCR (Fig. 1A), percentage of $Ccr10^{+}$ cells did not change significantly, suggesting that tissue culture conditions enhanced expression of Ccr10 only in a restricted population of MSCs.

Furthering attempts to identify chemotactic pathways that can be utilized for the recruitment of the MSCs to peripheral tissues, our extensive analysis of chemotactic molecules directly suggest that $Ccr1^{+}$MSCs can be recruited to various organs expressing multiple ligands of this receptor, whereas $Cxcr4^{+}$MSCs can be recruited only to organs with elevated expression of Cxcl12. Up to date, only few chemotactic axes, including CXCL12-CXCR4 and CCL21-CCR7, were tested for the ability to direct systemically transplanted MSCs to the skin (20). Although recruitment and therapeutic effects of $CXCR4^{+}$MSCs were reported, expression of CXCL12 in multiple organs did not provide desirable specificity leading to significant “dilution” of the therapeutic effect. This chemotactic axis was also shown to be responsible for the entrapment of systemically administered MSCs in lungs. Moreover, it was suggested that endogenously high level of CCL21 in secondary lymphoid organs was responsible for observed non-specific distribution of systemically transplanted MSCs (21). Populations of MSCs expressing Ccr4, Ccr6, Ccr9, and Ccr10 may provide a more targeted recruitment of these progenitors to specific tissues expressing cognate chemokines. However, $Ccr6^{+}$MSCs could be recruited toward inflamed tissues such as joints in rheumatoid arthritis by its unique ligand Ccl20 (22) and take part in restoration of damaged cartilage. Ccr9-expressing MSCs, especially after several passages *in vitro*, could migrate to intestine which secrets high levels of Ccl25, a unique ligand of Ccr9, and present there anti-inflammatory properties and alleviate symptoms associated with inflammatory diseases of intestine such as Crohn’s disease (19). Taking together, these observations strongly suggest that Ccr10-expressing MSCs could be recruited to epithelial tissues known to produce high levels of Ccl27 (23) and take part in its regeneration/repair. However, experimental proof for these hypotheses has yet to be obtained.

Our analyses also showed that *in vitro* culturing of MSCs results in down-regulation of many chemokines and receptors. These findings are in good agreement with prior observations showing that culturing of human MSCs beyond passage six resulted in a marked decrease Cxcr4 chemokine receptor and abrogation of chemotactic responsiveness of these cells to Cxcl12 (3). However, our studies also demonstrated that extended culturing not only influences on expression of chemokine receptors but also affects expression of chemokines. Thus, up-regulation of Ccl20, Ccl27 and Cxcl12 and concurrent expression of their cognate receptors in MSC^{cult} suggest the importance of these autocrine chemotactic

signals for propagation of MSCs *in vitro*. These observations also suggest that autocrine chemotactic signals may abrogate responsiveness of prolonged MSC culture to these chemokines *in vivo* after systemic transplantation.

Gene expression profile of chemokines and chemokine receptors in normal and EB-affected skin

Considering curative potential of MSCs in treatment of skin wounds (5, 12, 13), we examined the possibility that MSCs can be used as therapeutics for a group of hereditary mechanobullous skin disorders, collectively known as epidermolysis bullosa (EB). Our recent studies showed that localized transplantation of congenic MSCs into the skin of type VII collagen knock-out (KO) mice ($Col7a1^{-/-}$), which recapitulate human recessive dystrophic EB, counteracts the blistering phenotype (24). However taking into account inefficient homing of systemically transplanted MSCs to the skin, we suggested that paucity of MSCs in the skin can be explained by the absence of appropriate chemotactic signals recruiting circulating MSCs. To address this question, we examined expression of chemotactic molecules in the whole skin and in skin resident cells in normal and pathological conditions using wild-type (WT) mice and EB mouse models. The EB models consisted, in addition to $Col7a1^{-/-}$, of mice deficient in the laminin β3 ($Lamb3^{-/-}$) and laminin γ2 ($Lamc2^{-/-}$) mutants, respectively (15, 16). The latter mice recapitulate features of severe autosomal recessive junctional EB (JEB) in humans (25).

Microarray analysis of chemokine expression revealed that Ccl21a, Il-18, Ccl27, Ccl5, Cmtm8, Granulocyte-stimulating factor (Csf3), Cx3cl1, Cxcl14, Sdf2, and to lesser extent macrophage colony-stimulating factor (Csf1), granulocyte-macrophage colony-stimulating factor (Csf2), and Cmtm3 are expressed in WT skin with the highest expression of Ccl27, Csf3, Il-8, and Sdf2 (Table 2 and 3). Comparative analysis of chemokine expression in epidermal and dermal layers of the skin showed that Ccl27 is preferentially expressed in the epidermis (1.8 times higher than in dermis). Similar ratio was observed in primary mouse keratinocytes (PMK) and fibroblasts (PMF). This observation also was confirmed by semi-quantitative RT-PCR (Fig. 1B). Considering the fact that Ccl27 is predominantly expressed in epithelial tissues to recruit memory T cells as a part of immune surveillance mechanisms (26), it is plausible that Ccl27 chemokine may provide strongest chemotactic gradient for the recruitment of $Ccr10^{+}$MSCs to the skin.

In addition, preferential expression of several other chemokines and related molecules was observed in the epidermis. Expression of Ccrl1 was found to be epidermis-specific. As this receptor was shown to be involved in steady-state homing of leukocytes (27, 28), it is likely that its expression is associated with epidermal Langerhans cells (LC). Our array data also showed preferential expression of Cxcl14 and Il-18 in the epidermis. However, a more sensitive RT-PCR analysis demonstrated expression of both chemokines in epidermal and dermal components (Fig. 1B). As Cxcl14 was shown to be chemotactic to dendritic cells (DC) (29), it likely plays a significant role in retention of LC in the epidermis and recruitment of myeloid DC to the dermis as a part of immune surveillance. Similarly, Il-18, which stimulates production of IFN-γ, polarization of $CD4^{+}$ T-cell (30, 31) and immune-mediated bacterial clearance from the skin (32, 33), is also likely play a significant role in defense against skin infection. Consistent with this notion is the low expression of Ccrl1 and Cxcl14 in the epidermis of $Lamb3^{-/-}$ and $Lamc2^{-/-}$ null skin and correlative 3-times lower number of $CD11c^{+}$ APC in JEB skin. These finding suggest that susceptibility of the JEB patients to infection may be in part explained by the inefficient recruitment/retention of these immune sentinels in the skin.

Out of three colony-stimulating factors examined, Csf3 (GM-CSF) expression was on average 1.7 times higher in the whole epidermis than in the dermis. Conversely, Csf1 and

Csf2 (M-CSF and G-CSF, respectively) were expressed at low levels mostly in the dermis of WT and EB skin. This observation suggests a dual function of colony-stimulating factors in epidermal and dermal layers. In contrast to other chemokines, Cxcl4 (platelet factor 4) was highly expressed specifically in the dermis and detected in primary fibroblasts. Its expression was not detected in epithelial layer and PMK by means of array analysis, however, low level of expression was detected by RT-PCR (Fig. 1B). Cxcl4 chemokine is normally produced and released from activated platelets and it is chemotactic for neutrophils, fibroblasts and monocytes expressing a splice variant of the chemokine receptor Cxcr3, known as Cxcr3b (34). Therefore, it is likely that the majority of Cxcl4 derives from platelets and not from skin-residing cells. Cmtm3, a member of the CKLF-family of the MARVEL-domain-containing chemokines, was also preferentially expressed in the dermis and PMF. However, function of this chemokine is not yet known. Dermal-specific low level expression of Ccl21a was also observed by means of array and RT-PCR analyses. As Ccl21a is expressed by lymphatic vessels of the skin (35, 36), it is likely that it is primarily involved in mobilizing antigen-experience dendritic cells to regional lymph nodes rather than recruitment of various cell types from circulation to the skin. Expression of Ccl24 (eotaxin-2) was detected in a whole dermis and PMF. This chemokine is normally recruits eosinophils (37, 38).

Collectively, this wide-range of analyses showed that skin-derived chemotactic signals are preferentially involved in immune surveillance and steady-state homing of various immune cells to the skin rather than recruitment of the progenitors such as MSCs from circulation. Based on these findings, we suggest that skin-specific homing of therapeutic MSCs could be achieved via targeted alteration of chemotactic signals.

Migration of CCR10-expressing MSCs into normal skin after local and systemic administration

Direct matching of chemokine receptors expressed by MSCs with skin-derived chemokines suggests that CCL27-CCR10 chemotactic axis can provide efficient recruitment and homing of MSCs to the skin after systemic infusion. However, the presence of only a small percentage of Ccr10-expressing MSCs in the total pool of freshly cultured cells (Fig. 1C) and up-regulated production of CCL27 by prolonged MSC cultures (Fig. 1A) directly suggest that autocrine CCL27 may abrogate responsiveness of MSCs to the skin-derived chemokine. These findings also suggest that homing of systemically administered MSCs to the skin could be enhanced via the use of cells uniformly expressing CCR10 receptor.

In order to test this hypothesis, we generated minimally cultured MSCs overexpressing mouse Ccr10 (MSC^{Ccr10}) (Fig. 2A) and injected a mixture of fluorescently labeled MSC^{Ccr10} (red) and minimally cultured native MSCs (MSC^{min}/green) into the dermis of adult wild-type syngenic C57BL6/J mice. Subsequently, to provide a steep chemotactic gradient, 0.5 μg of recombinant mouse Ccl27 was injected ID at a site distal from the cell administration. One day later, both control MSC^{min} and MSC^{Ccr10} were found at the injection site as a mixture of green and red fluorescent signals (Fig 2B,E). During next five days, however, MSC^{Ccr10} progressively migrated from the site of injection and traveled through the skin along the Ccl27 chemotactic gradient (Fig. 2C,F,G). In contrast, MSC^{min} (green) mostly remained at the site of injection (Fig. 2D,H). When MSC^{Ccr10} cells were injected alone, similar pattern of distribution and intra-cutaneous migration was observed. One day after injection, localized red fluorescence was detected at MSC injection site (Fig 3A). After 7 days, high intensity fluorescence was detected at MSC injection site as well as near the site of chemokine administration (Fig. 3B). Remarkably, red fluorescent signals were observed throughout approximately 200 mm^2 area of examined skin. These observations suggest that after proteolytic degradation of injected Ccl27, the MSC^{Ccr10} cells continued lateral migration and populated a large area of the skin. Examination of the cross-

sections of the skin showed wide distribution of the FMDiI-labeled cells throughout examined area. Most of cellular migration occurred along the panniculus carnosus, a muscle layer which in mice underlies cutaneous tissue at the border of lower dermis and adipose tissue beneath hair bulb (Fig. 3D, E). Also, FMDiI-labeled MSC^{Ccr10} cells were detected in the upper dermis (Fig. 3F). In addition, histological examination of skin sections containing transplanted cells did not show any significant inflammatory infiltrate, suggesting that local chemokine administration does not result in significant inflammatory response. Collectively, these studies directly demonstrated that MSC^{Ccr10}population responded to the Ccl27 chemotactic gradient and that trafficking of MSCs though the skin can be regulated by Ccl27-Ccr10 chemotactic axis.

To examine whether Ccl27-Ccr10 chemotactic axis is suitable for the recruitment of systemically injected MSCs to the skin, FMDiI-labeled MSC^{Ccr10} and control native MSC^{min} cells were transplanted intravenously (IV) into adult syngenic C57BL6 mice, respectively. Following IV injection, 0.5 mg of recombinant Ccl27 was administered ID to a defined area of the dorsal skin. Mice were monitored for 8 days with repetitive administration of Ccl27 with 2 day intervals to provide constant localized chemotactic gradient. Despite continuous chemotactic gradient, control mice receiving FMDiI-labeled MSC^{min} did not show any significant accumulation of the transplanted cells at the site of chemokine administration (Fig. 4A). However, migration of transplanted MSC^{Ccr10} cells to the site of the Ccl27 administration was observed starting from day 1 (Fig. 4A). During a week, accumulation of fluorescent signals was observed in the majority of experimental mice which received MSC^{Ccr10} transplant. Immunofluorescent evaluation of the chemokine-treated skin confirmed very limited migration of MSC^{min} to the chemokine-treated area (Fig. 4B, C). A more significant accumulation of the MSC^{Ccr10} was observed in the lower dermis with some cells associated with blood vessels (Fig. 4D). In the mid and upper dermis, majority of MSC^{Ccr10} were located in the interfollicular dermis with some cells in a close proximity to the epidermis (Fig. 4E, F, G). Although varying degree of fluorescent signals was observed in mice receiving MSC^{Ccr10}, these *in vivo* studies confirmed Ccl27-mediated recruitment of the systemically administered Ccr10-expressing MSCs to the skin.

Most of our current knowledge on the chemotaxis-mediated recruitment of cells from circulation to cutaneous tissue comes from the studies on immune cell migration as the latter plays a significant role in immune surveillance and inflammatory response in the skin. At present, it is known that a combination of selectins and chemokines plays an important role in skin-specific T cell homing. For example, expression of L-selectin (CD62L) on the surface of leukocytes facilitates their attachment to ligands on high endothelial venules and non-lymphoid vascular endothelium and allows them to immigrate from circulation. Cytokine-dependent induction of E-selectins at the surface of the endothelium and expression of E-selectin ligands by leukocytes also play an essential role on leukocyte rolling and extravasation. Of particular interest to these studies is the observation that CD44, which is widely expressed on the surface of the bone-marrow derived MSCs, is a ligand for E-selectin that promotes the rolling interactions (39). Three chemokine receptors, CCR4, CCR6 and CCR10 expressed by memory T cells, were also shown to mediate T cell recruitment to the skin (26, 40, 41). Although contribution of each receptor to skin-specific trafficking is not well defined, it was suggested that interaction between CCR4 and its ligand CCL17 (TARC) on activated endothelial cells mediates T cell extravasation, whereas CCR10 further recruits these cells towards the skin epithelia. Taking into account this hypothesis and our current data on targeted migration of $Ccr10^{+}$MSCs toward and within the skin, it is likely that CCR10 alone may promote skin-targeted homing of systemically administered MSCs. However, as we detected variable degree of MSC^{Ccr10} recruitment after systemic administration, it is possible that expression of Ccr4 only in 18% of minimally

cultured MSCs (Fig. 1C) and different levels of inflammation-dependent E-selectin expression on endothelial cells may also affect recruitment of the MSC^{Ccr10} to the skin.

Overall, these studies demonstrate that Ccl27-Ccr10 chemotactic axis can be used to target systemically administered MSC^{Ccr10} to the skin providing wide-spread distribution of stem cells within cutaneous tissue. Our studies also suggest that further analysis of MSC subsets that express specific chemokine receptors such as Ccr4 and Ccr10, optimization of protocols for isolation of these subsets from the total pool of MSCs, and development of approaches providing uniform expression of these receptors in freshly isolated cells may further improve application of adult stem cells for the treatment of heritable skin disorders, such as EB.

Supplementary Material

Refer to Web version on PubMed Central for supplementary material.

Acknowledgments

We are grateful to Carol Kelly for assistance in preparing the manuscript. This work was supported in part by funds from the National Institute of Arthritis and Musculoskeletal and Skin Diseases, National Institutes of Health, and DEBRA International-DEBRA-Austria to OI, and by the Jefferson Medical College for VA.

Abbreviations

MSCs	mesenchymal stem cells
PMF	primary mouse fibroblasts
PMK	primary mouse keratinocytes
EB	epidermolysis bullosa
RDEB	recessive dystrophic epidermolysis bullosa
JEB	junctional epidermolysis bullosa
DEJ	dermal-epidermal junction
BMZ	basement membrane zone

References

1. Jackson WM, Nesti LJ, Tuan RS. Potential therapeutic applications of muscle-derived mesenchymal stem and progenitor cells. Expert Opin Biol Ther. 2010; 10:505–17. [PubMed: 20218920]
2. Bhakta S, Hong P, Koc O. The surface adhesion molecule CXCR4 stimulates mesenchymal stem cell migration to stromal cell-derived factor-1 in vitro but does not decrease apoptosis under serum deprivation. Cardiovasc Revasc Med. 2006; 7:19–24. [PubMed: 16513519]
3. Honczarenko M, Le Y, Swierkowski M, Ghiran I, Glodek AM, Silberstein LE. Human bone marrow stromal cells express a distinct set of biologically functional chemokine receptors. Stem Cells. 2006; 24:1030–41. [PubMed: 16253981]
4. Ringe J, Strassburg S, Neumann K, Endres M, Notter M, Burmester GR, et al. Towards in situ tissue repair: human mesenchymal stem cells express chemokine receptors CXCR1, CXCR2 and CCR2, and migrate upon stimulation with CXCL8 but not CCL2. J Cell Biochem. 2007; 101:135–46. [PubMed: 17295203]
5. Sasaki M, Abe R, Fujita Y, Ando S, Inokuma D, Shimizu H. Mesenchymal stem cells are recruited into wounded skin and contribute to wound repair by transdifferentiation into multiple skin cell type. J Immunol. 2008; 180:2581–7. [PubMed: 18250469]

6. Binger T, Stich S, Andreas K, Kaps C, Sezer O, Notter M, et al. Migration potential and gene expression profile of human mesenchymal stem cells induced by CCL25. Exp Cell Res. 2009; 15:1468–79. [PubMed: 19168060]
7. Kalwitz G, Endres M, Neumann K, Skriner K, Ringe J, Sezer O, et al. Gene expression profile of adult human bone marrow-derived mesenchymal stem cells stimulated by the chemokine CXCL7. Int J Biochem Cell Biol. 2009; 41:649–58. [PubMed: 18707017]
8. Grinnemo KH, Mansson A, Dellgren G, Klingberg D, Wardell E, Drvota V, et al. Xenoreactivity and engraftment of human mesenchymal stem cells transplanted into infarcted rat myocardium. J Thorac Cardiovasc Surg. 2004; 127:1293–300. [PubMed: 15115985]
9. Zhang J, Gong JF, Zhang W, Zhu WM, Li JS. Effects of transplanted bone marrow mesenchymal stem cells on the irradiated intestine of mice. J Biomed Sci. 2008; 15:585–94. [PubMed: 18763056]
10. Stich S, Haag M, Haupl T, Sezer O, Notter M, Kaps C, et al. Gene expression profiling of human mesenchymal stem cells chemotactically induced with CXCL12. Cell Tissue Res. 2009; 336:225–36. [PubMed: 19296133]
11. Wu Y, Chen L, Scott PG, Tredget EE. Mesenchymal stem cells enhance wound healing through differentiation and angiogenesis. Stem Cells. 2007; 25:2648–59. [PubMed: 17615264]
12. Chen L, Tredget EE, Wu PY, Wu Y. Paracrine factors of mesenchymal stem cells recruit macrophages and endothelial lineage cells and enhance wound healing. PLoS ONE. 2008; 3:e1886. [PubMed: 18382669]
13. Falanga V, Iwamoto S, Chartier M, Yufit T, Butmarc J, Kouttab N, et al. Autologous bone marrow-derived cultured mesenchymal stem cells delivered in a fibrin spray accelerate healing in murine and human cutaneous wounds. Tissue Eng. 2007; 13:1299–312. [PubMed: 17518741]
14. Heinonen S, Mannikko M, Klement JF, Whitaker-Menezes D, Murphy GF, Uitto J. Targeted inactivation of the type VII collagen gene (Col7a1) in mice results in severe blistering phenotype: a model for recessive dystrophic epidermolysis bullosa. J Cell Sci. 1999; 112 (Pt 21):3641–8. [PubMed: 10523500]
15. Meng X, Klement JF, Leperi DA, Birk DE, Sasaki T, Timpl R, et al. Targeted inactivation of murine laminin gamma2-chain gene recapitulates human junctional epidermolysis bullosa. J Invest Dermatol. 2003; 121:720–31. [PubMed: 14632187]
16. Kuster JE, Guarnieri MH, Ault JG, Flaherty LS, wiatek PJ. IAP insertion in the murine LamB3 gene results in junctional epidermolysis bullosa. Mamm Genome. 1997; 8:673–81. [PubMed: 9271670]
17. Flagler K, Alexeev V, Pierce EA, Igoucheva O. Site-specific gene modification by oligodeoxynucleotides in mouse bone marrow-derived mesenchymal stem cells. Gene Ther. 2008; 15:1035–48. [PubMed: 18337839]
18. Wynn RF, Hart CA, Corradi-Perini C, O'Neill L, Evans CA, Wraith JE, et al. A small proportion of mesenchymal stem cells strongly expresses functionally active CXCR4 receptor capable of promoting migration to bone marrow. Blood. 2004; 104:2643–5. [PubMed: 15251986]
19. Apostolaki M, Manoloukos M, Roulis M, Wurbel MA, Muller W, Papadakis KA, et al. Role of beta7 integrin and the chemokine/chemokine receptor pair CCL25/CCR9 in modeled TNF-dependent Crohn's disease. Gastroenterology. 2008; 134:2025–35. [PubMed: 18439426]
20. Sasaki M, Abe R, Fujita Y, Ando S, Inokuma D, Shimizu H. Mesenchymal stem cells are recruited into wounded skin and contribute to wound repair by transdifferentiation into multiple skin cell type. J Immunol. 2008; 180:2581–7. [PubMed: 18250469]
21. Cyster J. Leukocyte migration: scent of the T zone. Curr Biol. 2000; 10:R30–3. [PubMed: 10660291]
22. Hirota K, Yoshitomi H, Hashimoto M, Maeda S, Teradaira S, Sugimoto N, et al. Preferential recruitment of CCR6-expressing Th17 cells to inflamed joints via CCL20 in rheumatoid arthritis and its animal model. J Exp Med. 2007; 204:2803–12. [PubMed: 18025126]
23. Inokuma D, Abe R, Fujita Y, Sasaki M, Shibaki A, Nakamura H, et al. CTACK/CCL27 accelerates skin regeneration via accumulation of bone marrow-derived keratinocytes. Stem Cells. 2006; 24:2810–6. [PubMed: 16931770]

24. Alexeev V, Uitto J, Igoucheva O. Gene expression signatures of mouse bone marrow-derived mesenchymal stem cells in the cutaneous environment and therapeutic implications for blistering skin disorder. Cytotherapy. 2011; 13:30–45. [PubMed: 20854215]
25. Uitto J, McGrath JA, Rodeck U, Bruckner-Tuderman L, Robinson EC. Progress in epidermolysis bullosa research: toward treatment and cure. J Invest Dermatol. 2012; 130:1778–84. [PubMed: 20393479]
26. Homey B, Alenius H, Muller A, Soto H, Bowman EP, Yuan W, et al. CCL27-CCR10 interactions regulate T cell-mediated skin inflammation. Nat Med. 2002; 8:157–65. [PubMed: 11821900]
27. Comerford I, Milasta S, Morrow V, Milligan G, Nibbs R. The chemokine receptor CCX-CKR mediates effective scavenging of CCL19 in vitro. Eur J Immunol. 2006; 36:1904–16. [PubMed: 16791897]
28. Meurens F, Berri M, Auray G, Melo S, Levast B, Virlogeux-Payant I, et al. Early immune response following Salmonella enterica subspecies enterica serovar Typhimurium infection in porcine jejunal gut loops. Vet Res. 2009; 40:5. [PubMed: 18922229]
29. Salogni L, Musso T, Bosisio D, Mirolo M, Jala VR, Haribabu B, et al. Activin A induces dendritic cell migration through the polarized release of CXC chemokine ligands 12 and 14. Blood. 2009; 113:5848–56. [PubMed: 19339694]
30. Chakir H, Lam DK, Lemay AM, Webb JR. “Bystander polarization” of CD4+ T cells: activation with high-dose IL-2 renders naive T cells responsive to IL-12 and/or IL-18 in the absence of TCR ligation. Eur J Immunol. 2003; 33:1788–98. [PubMed: 12811838]
31. Schif-Zuck S, Westermann J, Netzer N, Zohar Y, Meiron M, Wildbaum G, et al. Targeted overexpression of IL-18 binding protein at the central nervous system overrides flexibility in functional polarization of antigen-specific Th2 cells. J Immunol. 2005; 174:4307–15. [PubMed: 15778395]
32. Srinivasan A, Salazar-Gonzalez RM, Jarcho M, Sandau MM, Lefrancois L, McSorley SJ. Innate immune activation of CD4 T cells in salmonella-infected mice is dependent on IL-18. J Immunol. 2007; 178:6342–9. [PubMed: 17475863]
33. Bohn E, Sing A, Zumbihl R, Bielfeldt C, Okamura H, Kurimoto M, et al. IL-18 (IFN-gamma-inducing factor) regulates early cytokine production in, and promotes resolution of, bacterial infection in mice. J Immunol. 1998; 160:299–307. [PubMed: 9551984]
34. Struyf S, Burdick MD, Proost P, Van Damme J, Strieter RM. Platelets release CXCL4L1, a nonallelic variant of the chemokine platelet factor-4/CXCL4 and potent inhibitor of angiogenesis. Circ Res. 2004; 95:855–7. [PubMed: 15459074]
35. Kodera M, Grailer JJ, Karalewitz AP, Subramanian H, Steeber DA. T lymphocyte migration to lymph nodes is maintained during homeostatic proliferation. Microsc Microanal. 2008; 14:211–24. [PubMed: 18312727]
36. Yoshino M, Yamazaki H, Nakano H, Kakiuchi T, Ryoke K, Kunisada T, et al. Distinct antigen trafficking from skin in the steady and active states. Int Immunol. 2003; 15:773–9. [PubMed: 12750361]
37. De Corso E, Baroni S, Romitelli F, Luca L, Di Nardo W, Passali GC, et al. Nasal lavage CCL24 levels correlate with eosinophils trafficking and symptoms in chronic sino-nasal eosinophilic inflammation. Rhinology. 2011; 49:174–9. [PubMed: 21743872]
38. Menzies-Gow A, Ying S, Sabroe I, Stubbs VL, Soler D, Williams TJ, et al. Eotaxin (CCL11) and eotaxin-2 (CCL24) induce recruitment of eosinophils, basophils, neutrophils, and macrophages as well as features of early- and late-phase allergic reactions following cutaneous injection in human atopic and nonatopic volunteers. J Immunol. 2002; 169:2712–8. [PubMed: 12193745]
39. Yago T, Shao B, Miner JJ, Yao L, Klopocki AG, Maeda K, et al. E-selectin engages PSGL-1 and CD44 through a common signaling pathway to induce integrin alphaLbeta2-mediated slow leukocyte rolling. Blood. 2010; 116:485–94. [PubMed: 20299514]
40. Campbell JJ, Haraldsen G, Pan J, Rottman J, Qin S, Ponath P, et al. The chemokine receptor CCR4 in vascular recognition by cutaneous but not intestinal memory T cells. Nature. 1999; 400:776–80. [PubMed: 10466728]

41. Homey B, Dieu-Nosjean MC, Wiesenborn A, Massacrier C, Pin JJ, Oldham E, et al. Up-regulation of macrophage inflammatory protein-3 alpha/CCL20 and CC chemokine receptor 6 in psoriasis. J Immunol. 2000; 164:6621–32. [PubMed: 10843722]

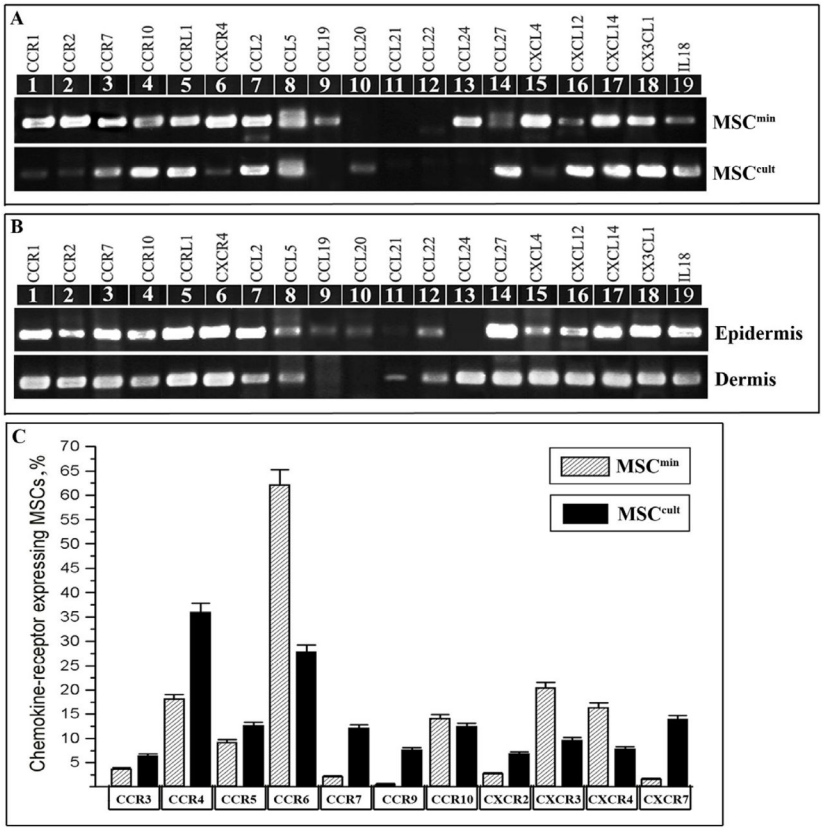

Figure 1.

The analysis of chemotactic molecules in MSCs, epidermal and dermal layers of the wild-type mouse skin. (A) Comparative RT-PCR-based assessment of receptors and chemokines in minimally cultured (MSC^{min}, p3) and prolonged cultured (MSC^{cult}, p 15) stem cells. (B) The RT-PCR analysis of selected receptors and chemokines in epidermal and dermal layers of the wild-type mouse skin. The analysis was carried out using gene-specific primers (Supplemental Table 1). (C) FACS-based analysis of selected chemokine receptors in MSC^{min} and MSC^{cult}. Data are presented as percentage of receptor-positive cells. The values are averages±SD for 3 replicates. Open bars depict MSC^{min} and filled bars MSC^{cult}.

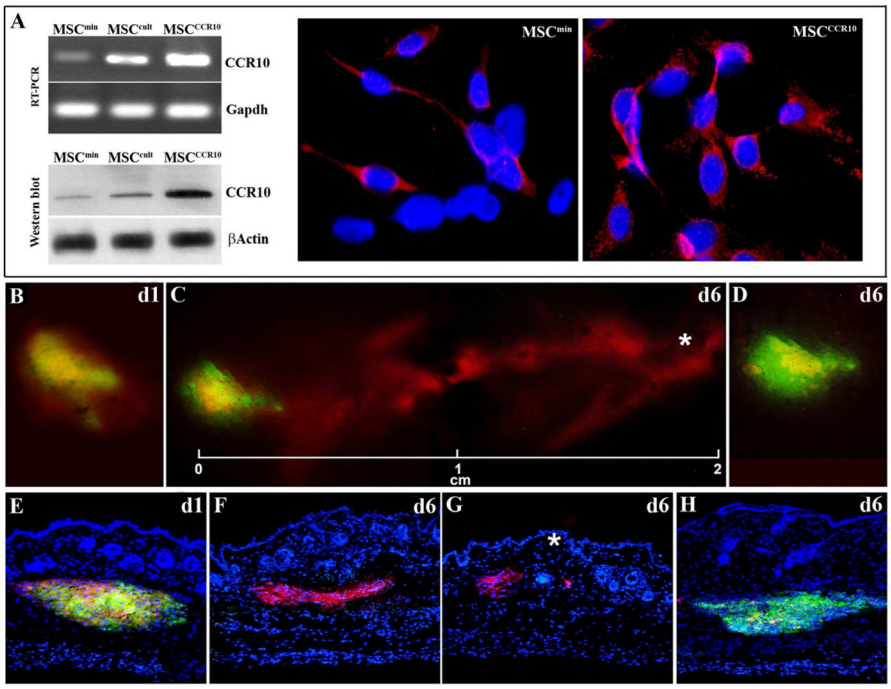

Figure 2.

Ccl27-mediated migration of MSC^{min} and MSC^{Ccr10} in the wild-type mouse skin. (A) Characterization of Ccr10 expression in minimally cultured (MSC^{min}, p3), prolonged cultured (MSC^{cult}, p 15), and minimally cultured Ccr10-overexpressing MSCs (MSC^{Ccr10}, p5) by RT-PCR, Western blot and immunofluorescent analyses. Ccr10 gene was amplified using gene-specific primers (Supplemental Table 1). The expression of *Gapdh* gene was used as an internal control. Western blot analysis was carried out using anti-mouse Ccr10 antibodies. The expression of β-actin was used as a loading control. The expression of Ccr10 in MSC^{min} and MSC^{Ccr10} was assessed by indirect immunofluorescence analysis using Ccr10-specific antibodies (red). Nuclei were counterstained with DAPI (blue). (B–D) Direct fluorescent imaging of mouse dorsal skin transplanted with a mixture (1:1) of MSC^{min} (green) and MSC^{Ccr10} (red) cells at day 1 (B) and day 6 (C and D) after transplantation. Migration of MSC^{Ccr10} was detected by distribution of red fluorescence from original site of cell injection (mixture of green and red signals, B) to the site of Ccl27 administration (indicated with an asterisk). Distance (cm) between cell transplantation site and Ccl27 administration site is indicated on panel C. (E-H) Direct fluorescence detection of transplanted MSC^{min} (green) and MSC^{Ccr10} (red) cells on cryosections (7 μm) at day 1 (E) and day 6 (F–H) after transplantation. Time points (d) indicated at right top corners of the panels. Asterisk indicates the site of Ccl27 injection. Nuclei were counterstained with DAPI (blue).

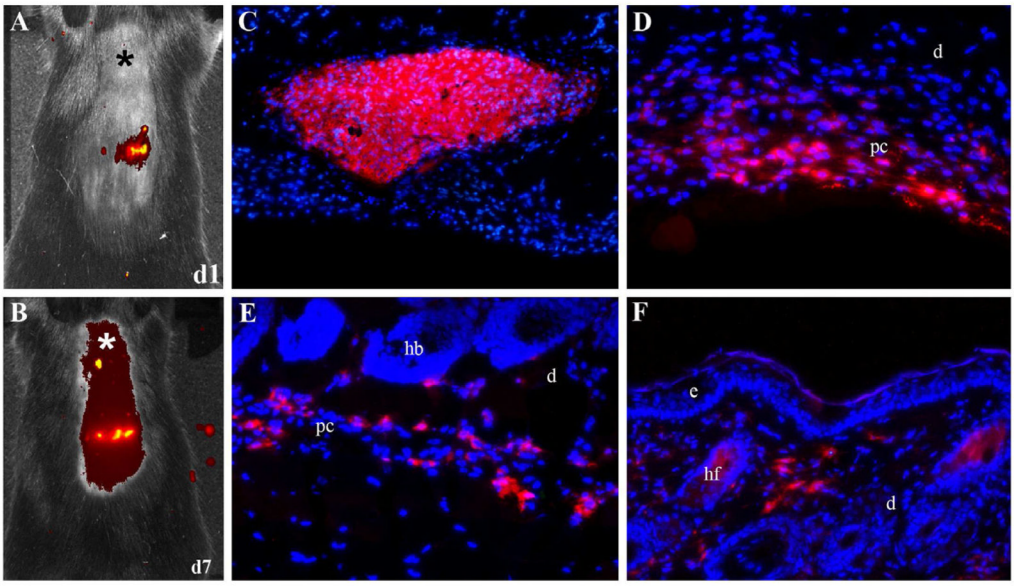

Figure 3.

Live-imaging of Ccl27-mediated migration of locally transplanted MSC^{Ccr10} in the wild-type mouse skin. Transplanted cells (red) in the mouse skin were detected at day 1 (A) and day 7 (B) using IVIS imaging system. Before analysis, the mouse skin was depilated to allow detection of fluorescent signals. Asterisks indicate the site of Ccl27 injection. (C–F) Direct fluorescence detection of transplanted MSC^{Ccr10} (red) on cryosections (7 μm) at days 1 (C) and 7 (D–F) after transplantation. Nuclei were counterstained with DAPI (blue). e - epidermis; d – dermis; hf - hair follicle; hb - hair bulb; pc - panniculus carnosus. Scale bar - 100 μm.

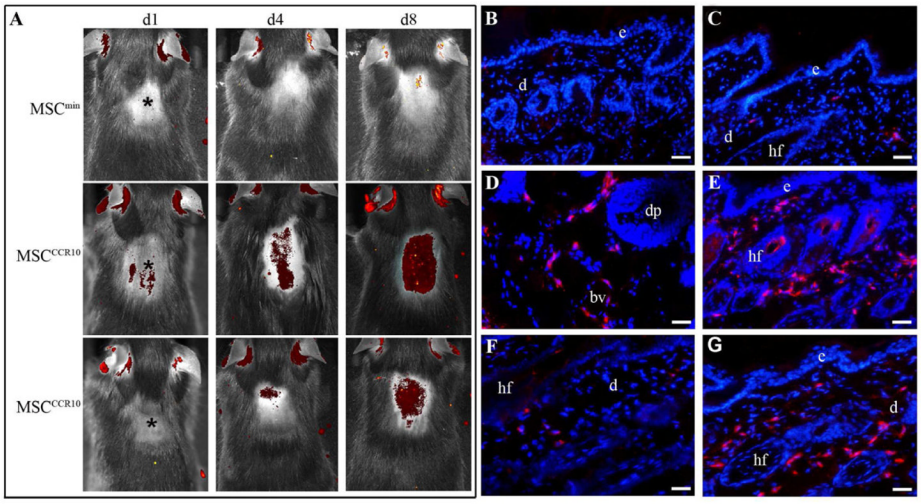

Figure 4.

Live-imaging of Ccl27-mediated recruitment of systemically transplanted MSC^{min} and MSC^{Ccr10} to the skin. (A) The wild-type mice were transplanted with stem cells via tail vein injection followed by intradermal injections of Ccl27. Assessment of cell recruitment (red fluorescence) to the skin was done at day 1, 4, and 8, respectively. Time points (d) indicated at top of the panels. Variations in migration efficiency of MSC^{Ccr10} are depicted by presentation of two experimental mice with different degree of transplants in the skin. Asterisks indicate the site of Ccl27 administration. Direct fluorescent images of representative skin cryosections (7 μm) from MSC^{min} (B, C) and MSC^{Ccr10} infused mice (D-G). e - epidermis; d – dermis; hf - hair follicle; bv - blood vessel; dp – dermal papilla. Nuclei were counterstained with DAPI (blue). Scale bar - 100 μm.

Cytotherapy. Author manuscript; available in PMC 2014 February 01.

Table 1

Gene expression analysis of chemokines and receptors in primary MSC cultures.

RefSeq Number	Gene	Description	MSC^{min}	MSC^{cult}	Fold difference[a]
NM_011784	Agtrl1	Angiotensin receptor-like 1	265.0	245.0	1.1
NM_021609	Ccbp2	Chemokine binding protein 2	149.00	139.00	1.1
NM_009912	Ccr1	Chemokine (C-C motif) receptor 1	500.00	80.00	6.3
NM_009915	Ccr2	Chemokine (C-C motif) receptor 2	500.00	95.00	5.3
NM_009914	Ccr3	Chemokine (C-C motif) receptor 3	43.00	51.00	0.8
NM_009916	Ccr4	Chemokine (C-C motif) receptor 4	120.00	270.00	0.4
NM_009917	Ccr5	Chemokine (C-C motif) receptor 5	98.00	100.00	1.0
NM_009835	Ccr6	Chemokine (C-C motif) receptor 6	157.00	72.00	2.2
NM_007719	Ccr7	Chemokine (C-C motif) receptor 7	300.00	212.00	1.4
NM_009913	Ccr9	Chemokine (C-C motif) receptor 9	25.00	35.00	0.7
NM_145700	Ccrl1	Chemokine (C-C motif) receptor-like 1	400.00	410.00	1.0
NM_009910	Cxcr3	Chemokine (C-X-C motif) receptor 3	120.00	69.00	1.7
NM_009911	Cxcr4	Chemokine (C-X-C motif) receptor 4	500.00	73.00	6.8
NM_007722	Cxcr7	Chemokine (C-X-C motif) receptor 7	50.00	89.00	0.6
NM_011329	Ccl1	Chemokine (C-C motif) ligand 1	210.10	210.10	1.0
NM_011333	Ccl2	Chemokine (C-C motif) ligand 2	555.00	545.00	1.0
NM_013653	Ccl5	Chemokine (C-C motif) ligand 5	290.00	280.00	1.0
NM_013654	Ccl7	Chemokine (C-C motif) ligand 7	52.21	52.21	1.0
NM_011888	Ccl19	Chemokine (C-C motif) ligand 19	50.00	0.00	only MSC^{min}
NM_016960	Ccl20	Chemokine (C-C motif) ligand 20	0.00	30.00	only MSC^{cult}
NM_019577	Ccl24	Chemokine (C-C motif) ligand 24	513.00	0.00	only MSC^{min}
NM_011336	Ccl27	Chemokine (C-C motif) ligand 27	44.00	427.00	0.1
NM_009140	Cxcl2	Chemokine (C-X-C motif) ligand 2	64.00	559.00	0.1
NM_019932	Cxcl4	Chemokine (C-X-C motif) ligand 4	510.00	37.00	13.8
NM_021704	Cxcl12	Chemokine (C-X-C motif) ligand 12	62.00	462.00	0.1
NM_018866	Cxcl13	Chemokine (C-X-C motif) ligand 13	17.00	20.00	0.9

RefSeq Number	Gene	Description	MSC^{min}	MSC^{cult}	Fold difference[a]
NM_019568	Cxcl14	Chemokine (C-X-C motif) ligand 14	429.00	512.00	0.8
NM_009142	Cx3cl1	Chemokine (C-X3-C motif) ligand 1	355.00	555.00	0.6
NM_024217	Cmtm3	CKLF-like MARVEL transmembrane domain containing 3	526.1	549.0	1.0
NM_133978	Cmtm7	CKLF-like MARVEL transmembrane domain containing 7	491.8	468.0	1.1
NM_007778	Csf1	Colony stimulating factor 1 (macrophage)	561.8	545.0	1.0
NM_010431	Hif1a	Hypoxia inducible factor 1, alpha subunit	204.6	224.6	0.9
NM_008360	Il18	Interleukin 18	474.2	574.2	0.8
NM_008610	Mmp2	Matrix metallopeptidase 2	561.8	582.8	1.0
NM_010851	Myd88	Myeloid differentiation primary response gene 88	379.7	297.0	1.3
NM_008689	Nfkb1	Nuclear factor of kappa light chain gene enhancer in B-cells 1, p105	358.5	318.5	1.1
NM_007926	Scye1	Small inducible cytokine subfamily E, member 1	423.6	394.6	1.1
NM_009143	Sdf2	Stromal cell derived factor 2	552.8	512.8	1.1

[a]The fold difference represents the ratio of intensity of each gene hybridized with the RNA isolated from minimally cultured MSC (MSC^{min}) normalized to the intensity of the corresponding gene from prolong cultured MSC (MSC^{cult}). Each array was processed in an identical manner and the number represents an average of triplicate experiments from three independent isolations. Each gene is demarcated by the RefSeq accession number, a description of the gene and its common name.

Table 2

Gene expression analysis of chemokines and receptors in epidermis of wild-type and EB mice and primary keratinocytes.

			Fold difference			
RefSeq number	**Symbol**	**Description**	**LamC2/wt[a]**	**LamB3/wt[a]**	**Col7a1/wt[a]**	**PMK/wt[a]**
NM_011336	Ccl27	Chemokine (C-C motif) ligand 27	1.04	0.64	0.50	0.93
NM_013653	Ccl5	Chemokine (C-C motif) ligand 5	0.58	0.45	1.72	ND
NM_145700	Ccrl1	Chemokine (C-C motif) receptor-like 1	0.49	0.45	0.57	ND
NM_133978	Cmtm7	CKLF-like MARVEL transmembrane domain containing 7	ND	ND	ND	only PMK
NM_027294	Cmtm8	CKLF-like MARVEL transmembrane domain containing 8	0.39	1.29	0.63	ND
NM_007722	Cxcr7	Chemokine (C-X-C motif) receptor 7	ND	ND	ND	only PMK
NM_009969	Csf2	Colony stimulating factor 2 (granulocyte-macrophage)	ND	ND	ND	only PMK
NM_009971	Csf3	Colony stimulating factor 3 (granulocyte)	0.31	0.79	1.06	0.32
NM_009142	Cx3cl1	Chemokine (C-X3-C motif) ligand 1	0.25	0.37	0.67	2.13
NM_019568	Cxcl14	Chemokine (C-X-C motif) ligand 14	0.65	0.67	0.77	ND
NM_023158	Cxcl16	Chemokine (C-X-C motif) ligand 16	ND	ND	ND	only PMK
NM_008360	Il18	Interleukin 18	1.16	1.24	1.08	ND
NM_010564	Inha	Inhibin alpha	0.94	0.75	1.17	ND
NM_010851	Myd88	Myeloid differentiation primary response gene 88	0.77	1.18	0.66	1.05
NM_007926	Scye1	Small inducible cytokine subfamily E, member 1	ND	ND	ND	only PMK
NM_009143	Sdf2	Stromal cell derived factor 2	0.85	0.85	0.67	2.14

[a]The fold difference represents the ratio of intensity of each gene hybridized with the RNA isolated from epidermis of LamC2, LamB3, Col7a1or primary keratinocytes (PMK) normalized to the intensity of the corresponding gene from epidermis of wild-type (wt) mouse, respectively. Each array was processed in an identical manner and the number represents an average of triplicate experiments from three independent isolations. Each gene is demarcated by the RefSeq accession number, a description of the gene and its common name. ND, not detected.

Table 3

Gene expression analysis of chemokines and receptors in dermis of wild-type and EB mice and primary fibroblasts.

			Fold difference			
RefSeq number	**Symbol**	**Description**	**LamC2/wt[a]**	**LamB3/wt[a]**	**Col7a1/wt[a]**	**PMF/wt[a]**
NM_030711	Arts1	Type 1 tumor necrosis factor receptor shedding aminopeptidase regulator	only wt	only wt	only wt	only wt
NM_007540	Bdnf	Brain derived neurotrophic factor	only wt	only wt	only wt	only wt
NM_007556	Bmp6	Bone morphogenetic protein 6	only wt	only wt	only wt	only wt
NM_011330	Ccl11	Small chemokine (C-C motif) ligand 11	only wt	only wt	only wt	only wt
NM_011888	Ccl19	Chemokine (C-C motif) ligand 19	0.72	0.58	0.53	ND
NM_011333	Ccl2	Chemokine (C-C motif) ligand 2	0.62	0.66	0.66	0.25
NM_011335	Ccl21a	Chemokine (C-C motif) ligand 21a	0.84	0.66	0.78	0.76
NM_019577	Ccl24	Chemokine (C-C motif) ligand 24	0.72	0.68	0.95	0.28
NM_011336	Ccl27	Chemokine (C-C motif) ligand 27	1.10	0.68	0.70	1.32
NM_021443	Ccl8	Chemokine (C-C motif) ligand 8	only wt	only wt	only wt	only wt
NM_009912	Ccr1	Chemokine (C-C motif) receptor 1	only wt	only wt	only wt	only wt
NM_009915	Ccr2	Chemokine (C-C motif) receptor 2	1.05	0.99	1.01	ND
NM_145700	Ccrl1	Chemokine (C-C motif) receptor-like 1	0.61	0.60	0.61	0.41
NM_024217	Cmtm3	CKLF-like MARVEL transmembrane domain containing 3	0.75	0.73	0.69	1.59
NM_026036	Cmtm6	CKLF-like MARVEL transmembrane domain containing 6	0.74	0.63	0.84	0.70
NM_133978	Cmtm7	CKLF-like MARVEL transmembrane domain containing 7	0.62	0.58	0.58	1.45
NM_027294	Cmtm8	CKLF-like MARVEL transmembrane domain containing 8	0.84	0.72	0.66	1.37
NM_008153	Cmklr1	Chemokine-like receptor 1	0.95	0.73	0.95	ND
NM_007722	Cxcr7	Chemokine (C-X-C motif) receptor 7	0.57	0.49	0.73	1.45
NM_007778	Csf1	Colony stimulating factor 1 (macrophage)	0.63	0.68	1.07	1.28
NM_009969	Csf2	Colony stimulating factor 2 (granulocyte-macrophage)	0.48	0.45	0.38	1.85
NM_009971	Csf3	Colony stimulating factor 3 (granulocyte)	1.03	1.61	2.75	ND
NM_009142	Cx3cl1	Chemokine (C-X3-C motif) ligand 1	0.58	0.39	0.26	1.38
NM_009987	Cx3cr1	Chemokine (C-X3-C) receptor 1	ND	ND	ND	only PMF
NM_021274	Cxcl10	Chemokine (C-X-C motif) ligand 10	1.01	0.99	1.03	ND
NM_021704	Cxcl12	Chemokine (C-X-C motif) ligand 12	0.81	0.81	0.92	ND

			Fold difference			
RefSeq number	**Symbol**	**Description**	**LamC2/wt[a]**	**LamB3/wt[a]**	**Col7a1/wt[a]**	**PMF/wt[a]**
NM_018866	Cxcl13	Chemokine (C-X-C motif) ligand 13	0.70	0.71	0.71	ND
NM_019568	Cxcl14	Chemokine (C-X-C motif) ligand 14	0.71	0.71	0.98	1.72
NM_023158	Cxcl16	Chemokine (C-X-C motif) ligand 16	0.70	0.55	0.75	ND
NM_009140	Cxcl2	Chemokine (C-X-C motif) ligand 2	0.77	0.72	0.94	ND
NM_019932	Cxcl4	Chemokine (C-X-C motif) ligand 4	0.89	0.82	0.74	0.34
NM_009911	Cxcr4	Chemokine (C-X-C motif) receptor 4	0.73	0.53	0.45	ND
NM_010045	Darc	Duffy blood group, chemokine receptor	0.55	0.55	0.55	ND
NM_138302	Ecgf1	Endothelial cell growth factor 1 (platelet-derived)	0.97	0.97	1.02	ND
NM_175520	Gpr81	G protein-coupled receptor 81	0.77	0.69	0.77	ND
NM_010431	Hif1a	Hypoxia inducible factor 1, alpha subunit	0.70	0.72	0.71	0.92
NM_008360	Il18	Interleukin 18	0.59	0.70	0.57	0.56
NM_021283	Il4	Interleukin 4	0.82	0.82	1.09	ND
NM_010564	Inha	Inhibin alpha	1.04	1.01	1.02	1.41
NM_008381	Inhbb	Inhibin beta-B	0.66	0.66	0.73	0.37
NM_008610	Mmp2	Matrix metallopeptidase 2	0.72	0.76	0.91	1.53
NM_010851	Myd88	Myeloid differentiation primary response gene 88	0.82	0.68	0.56	1.29
NM_008689	Nfkb1	Nuclear factor of kappa light chain gene enhancer in B-cells 1, p105	0.53	0.53	0.52	1.30
NM_019492	Rgs3	Regulator of G-protein signaling 3	1.04	0.76	0.77	ND
NM_007926	Scye1	Small inducible cytokine subfamily E, member 1	0.59	0.69	0.76	1.57
NM_009143	Sdf2	Stromal cell derived factor 2	1.07	1.04	0.50	1.60
NM_178804	Slit2	Slit homolog 2 (Drosophila)	0.72	0.62	0.74	0.72
NM_021297	Tlr4	Toll-like receptor 4	1.07	0.84	1.08	ND
NM_013693	Tnf	Tumor necrosis factor	0.52	0.71	0.53	ND

[a]The fold difference represents the ratio of intensity of each gene hybridized with the RNA isolated from dermis of LamC2, LamB3, Col7a1or primary fibroblasts (PMF) normalized to the intensity of the corresponding gene from dermis of wild-type (wt) mouse, respectively. Each array was processed in an identical manner and the number represents an average of triplicate experiments from three independent isolations. Each gene is demarcated by the RefSeq accession number, a description of the gene and its common name. ND, not detected.